

**DESIGN OF LOW NOISE AMPLIFIER FOR  
ULTRA-WIDEBAND (UWB) APPLICATIONS  
USING SILTERRA 0.18  $\mu\text{m}$  CMOS TECHNOLOGY**

**Oleh**

**Ooi Wei Ching**

**Disertasi ini dikemukakan kepada  
UNIVERSITI SAINS MALAYSIA**

**Sebagai memenuhi sebahagian daripada syarat keperluan  
untuk ijazah dengan kepujian**

**SARJANA MUDA KEJURUTERAAN (KEJURUTERAAN ELEKTRONIK)**

**Pusat Pengajian Kejuruteraan  
Elektrik dan Elektronik  
Universiti Sains Malaysia**

**Mei 2006**



## Abstrak

Penguat hingar rendah dengan aplikasi bagi sistem “Ultra-wideband (UWB)” telah dijalankan dalam projek ini. Rekabentuk penguat ini hanya menggunakan fasa pertama bagi sistem UWB, di mana lingkungan frekuensi adalah dari 3.1 GHz hingga 4.9 GHz. Ciri-ciri isyarat UWB dan sistem UWB diterangkan dalam disertasi ini. Untuk memenuhi ciri-ciri bagi isyarat UWB, rekabentuk penguat dijalankan dengan menggunakan proses CMOS 0.18  $\mu\text{m}$  daripada Silterra. Melalui teknologi ini, jumlah arus digunakan dalam rekabentuk ini mencatatkan 5.9 mA dan kuasa pembekal yang diperlukan ialah 1.8 V. Topologi yang dipilih untuk rekabentuk penguat hingar rendah ialah penguat “inductively degenerated common source”. Topologi ini biasanya terkenal dalam aplikasi untuk sistem “narrow band”. Oleh itu, langkah pembaikan diperlukan agar topologi ini sesuai untuk aplikasi bagi UWB. Hal ini dapat dicapai dengan bantuan penuras bebas jalur. Sehubungan itu, rekabentuk telah dijalankan dalam 2 versi di mana induktor yang ideal dan praktik masing-masing digunakan untuk tujuan perbandingan. Daripada prestasi yang tercatat, gandaan sebanyak 14.1 dB dengan toleransi sebanyak  $\pm 0.25$  dB tercapai, hingar yang kurang daripada 2.9 dB diperolehi serta kelinearan daripada IIP3 mencatatkan -6.2 dBm apabila penguat hingar rendah direkabentuk dengan induktor yang ideal. Walau bagaimanapun, sedikit kejatuhan sebanyak 0.9 dB didapati dalam gandaan apabila rekabentuk penguat ini menggunakan induktor yang praktik. Tambahan pula, hingar yang didapati menjadi lebih tinggi, iaitu sebanyak 6 dB. Daripada simulasi, kuasa lesapan bagi penguat yang menggunakan baik induktor yang ideal mahupun induktor yang praktik mencatatkan 10.6 mW dan 11.25 mW masing-masing. Di samping itu, penguat hangar rendah yang menggunakan induktor yang praktik, disediakan oleh Silterra, SIL18RF juga disimulasikan. Daripada simulasi, kejatuhan gandaan kepada 8.5 dB diperolehi, hingar rendah iaitu sebanyak 4.3 dB dicatatkan. Sehubungan itu, size induktor SIL18RF yang besar menyebabkan die yang besar diperlukan. Pengukuran bagi MAX 2654 kit dengan menggunakan alatan canggih yang terdapat dalam makmal perhubungan juga disertakan dalam projek ini. Didapati gandaan sebanyak 9 dB diperolehi dan kuasa lesapan mencatatkan nilai 15 mW.

## Abstract

The low noise amplifier (LNA) for Ultra Wideband (UWB) mode 1 application, which is covering a frequency range from 3.1 GHz to 4.9 GHz. LNA is the first gain element in the receiver architecture. It is designed for Direct Conversion (DICON). Based on these system characteristics, inductive degenerated common source LNA was designed using Silterra 0.18  $\mu\text{m}$  process. UWB system with multi band Orthogonal Frequency Division Multiplexing (MBOA) was chosen over Direct Sequence Spread Spectrum (DSSS) due to its full optimization of the allocated 7.5 GHz bandwidth. This LNA consumes 5.9 mA of total current from a 1.8 V dc power supply. LNA is designed using inductive degenerated common source amplifier, which is widely used in narrow band design. For UWB application such as wideband matching was implemented to extend the bandwidths of a narrow band system. In this project, wideband reactive matching following by *LC* Chebyshev band pass filter is utilized. The *LC* band pass filter utilizes the transformation from low pass network to band pass network is presented. Impedance and frequency scaling are used in filter transformation from a low pass filter to a band pass filter. The wideband filter, as input matching network, is designed on chip for better integration. Three test cases were carried out using LNA with ideal inductors, ASITIC inductors and SIL18RF inductors. For the ideal LNA, higher power consumption of 11.25 mW is observed at 1.9 GHz bandwidth, 14.1 dB power gain with gain flatness of  $\pm 0.25$  dB, input and output match of -10 dB over its frequency range, noise figure of 2.9 dB and third order intercept point of -6.2 dBm with ideal inductors is . However, using ASITIC inductor, the gain of LNA is dropped to 13.2 dB with gain flatness of  $\pm 1.5$  dB exhibiting higher noise figure of less than 6 dB with the same input and output matching and comparable third order intercept point. On the other hand, using SIL18RF inductor, the gain of LNA is further decreased to 8.5 dB, exhibiting noise figure of less than 4.3 dB with poorer input and output matching of -9.5 dB and -6.1 dB, respectively. Measurements were carried out on MAX 2654 evaluation kit at a frequency scaling of 1.6 GHz, exhibiting a 9 dB gain, input and output match of -7 dB and -14 dB, respectively and higher power consumption, 15 mW.

### **Acknowledgements**

I would like to take this opportunity to express my gratitude towards certain respectable individuals for their consistent assistance, guidance, and support, in terms of technical advice as well as emotional and moral support.

First, I would like to express my sincere thanks to my supervisor, Dr. Tun Zainal Azni Zulkifli who gave me a good opportunity to get myself involve in the cutting-edge UWB research programme. I would like to thank Dr. Tun again for taking time off from his busy schedule to educate his students on this particular research. His invaluable guidance and insight has given me a good exposure and interest in this final year project. His opinions and suggestions have been very invaluable in debugging, as well as improving my circuit. His great efforts and sacrifices in bringing us to experience the industrial standard CAD tools and design kits, as well as to fabricate my LNA integrated circuit. Moreover, I would like to thank Dr. Tun Zainal Azni Zulkifli for his patience in seeing this dissertation through all the trials and tribulations.

My gratitude also goes towards Puan Norlaili Bt. Mohd. Noh for her outstanding support and assistance with the technical aspects during the effort of the Low Noise Amplifier (LNA) design. I am also indebted to Mr. Tan Yee Chyan, Mr Harikrishnan Rahmiah, postgraduate students, for their guidance in the CAD tools as well as valuable comments in debugging and improving my circuit. Their helps and ideas are much appreciated.

Also deserving of my appreciations are Mr.Yap Hock Lian, Mr. Moh Kim Hock, Mr. Khor Boon Tiang, all who have been very helpful to me during the process of this work being completed. Their invaluable discussions and assistances as well as sharing with the technical aspects are much appreciated.

Next, I would like to thank the people who were most responsible for providing both moral support and much enjoyment outside of school, helping me to keep me sane throughout this process. These people include my roommate, Miss Yeoh Ee Ee as well my friends, Miss Lee Swee Wah, Miss Lily Tiong You Wen and Miss Neoh Chai Chen.

Finally yet importantly, I wish to express my gratitude to my family for their support throughout the years. Without their support, I most certainly could not have come this far. They have been extremely important for helping me accomplishing through the highs and lows of this research project.

## Table of Contents

	<b>PAGE</b>
<b>ABSTRACT</b>	<b>i</b>
<b>ACKNOWLEDGEMENT</b>	<b>iii</b>
<b>TABLE OF CONTENT</b>	<b>iv</b>
<b>LIST OF FIGURES</b>	<b>vii</b>
<b>LIST OF TABLES</b>	<b>x</b>
<b>CHAPTER 1 INTRODUCTION</b>	
1.1 Introduction to Ultra-Wide Bandwidth (UWB) Technology	1
1.2 Objective	3
1.3 Design Flow	4
1.4 Project Overview	5
<b>CHAPTER 2 BASIC FOR ULTRA-WIDE BANDWIDTH AND RF FUNDAMENTALS</b>	
2.1 UWB Technology	8
2.2 Approach of UWB System	11
2.2.1 Multi-band Approach	11
2.3 RF Fundamentals	14
2.3.1 Impedance Matching	14
2.3.2 Linearity	16
2.3.2.1 1-dB Compression Point ( $P_{1dB}$ )	16
2.3.2.2 Third Order Intercept (IIP3)	17
<b>CHAPTER 3 UWB RECEIVER ARCHITECTURE</b>	
3.1 Overview of UWB System	20
3.2 Requirements of Receiver	21
3.3 Direct Conversion Architecture (DICON)	22
3.4 Comparison between Direct Conversion (DICON) and Superheterodyne	27
<b>CHAPTER 4 LOW NOISE AMPLIFIER</b>	
4.1 Common Goals of LNA	29
4.2 Technology	30
4.3 Existing Topologies of Low Noise Amplifier	30
4.3.1 Resistive Termination	32

4.3.2	Common Gate Amplifier	33
4.3.3	Shunt-Series Feedback Amplifier	34
4.3.4	Inductively Degenerated Common Source Amplifier	34
4.3.5	Distributed Amplifier	35
4.3.6	Balanced Amplifier	36
4.3.7	Comparison among LNA Topologies	37
4.4	Wideband Impedance Matching Network	38
4.5	Architectures of low noise amplifier	41
4.5.1	Single-ended over Differential architecture	41
4.5.2	Cascode Stage Amplifier	43
4.6	Passive Elements	45
4.6.1	Resistors	45
4.6.2	Inductors	45
4.7	Design Procedure	47

## **CHAPTER 5           CIRCUIT ANALYSIS OF DESIGNED LOW NOISE AMPLIFIER FOR UWB APPLICATION**

5.1	Low Noise Amplifier (LNA) Analysis	49
5.2	Input Matching Network	51
5.3	Wideband Impedance Matching	54
5.4	Gain Enhancement Technique	59
5.5	Linearity	62
5.6	Noise Analysis	63
5.7	Current Budget	65
5.8	Biasing Technique	65

## **CHAPTER 6           SIMULATION RESULTS AND DISCUSSIONS**

6.1	DC Analysis	69
6.1.1	Device Size	72
6.1.2	Biasing Circuitry	73
6.1.3	Supply Voltage and Temperature Sensitivity	75
6.1.4	Power Consumption	77
6.2	S-Parameter Analysis	79
6.2.1	Ideal Simulation	80
6.2.2	Comparison among three sub-band in UWB mode 1 application	87
6.2.3	Actual simulation	91
6.2.4	Comparison between Ideal and Actual Simulation	101
6.3	Periodic-Steady-State (PSS) Analysis	104
6.3.1	1 dB Compression Point	105
6.3.2	Third Order Intercept Point (IP3)	115
6.4	Summary	118

<b>CHAPTER 7</b>	<b>LAYOUT</b>	
7.1	Layout Overview	122
7.2	Layout Precautions	123
7.3	Design Flow in Layout	124
7.4	Layout of Low Noise Amplifier (LNA) Design	125
	7.4.1 Square Shunt ASITIC Inductor	125
	7.4.2 POLY SILICON PATTERN GROUND SHIELD DESIGN	125
	7.4.3 BONDING PAD DESIGN	127
	7.4.4 Layout of LNA with SIL18RF Inductor	128
	7.4.5 Improved Layout of LNA with ASITIC Inductor	128
7.5	Results in Verification	128
	7.5.1 Design Rule Check (DRC)	128
	7.5.2 Extraction	131
	7.5.3 Layout Versus Schematic (LVS)	131
<b>CHAPTER 8</b>	<b>HARDWARE CHARACTERIZATION</b>	
8.1	General Description on MAX2654 Evaluation Kit	132
8.2	Test Equipments	135
8.3	Specifications of MAX 2654	136
8.4	Methodology	136
	8.4.1 Network Analyzer	137
	8.4.2 RF Spectrum Analyzer	139
	8.4.3 RF Signal Generator	139
8.5	Measurement Results	142
	8.5.1 DC biasing	142
	8.5.2 Scattering Parameter (SP)	143
	8.5.3 Input 1dB Compression Point	149
8.6	Discussion	151
8.7	PCB Layout	152
	8.7.1 Calculation	153
<b>CHAPTER 9</b>	<b>CONCLUSIONS AND FUTURE WORKS</b>	
9.1	Future Works	155
9.2	Comparison With Works Done By Others	155
9.3	Conclusions	155
<b>REFERENCES</b>		158

## LIST OF FIGURES

	PAGE
Fig. 1.1: Band plan in Mode 1 UWB application	3
Fig. 1.2: Design Flow of this project	6
Fig. 2.1: Band plan of multi band OFDM	12
Fig. 2.2: A lossless matching network	15
Fig. 2.3: The dynamic range of system from input and output power relation	17
Fig. 2.4: The Third Order Intercept point (IP3)	19
Fig. 3.1: Direct Conversion (DICON) Receiver Architecture	22
Fig. 4.1: Common LNA topologies, (a) Resistive termination, (b) $1/g_m$ termination, (c) shunt-series feedback, (d) inductive degeneration, (e) distributed amplifiers and (f) balanced amplifiers.	31
Fig. 4.2: Sixth order <i>LC</i> band pass filter	39
Fig. 4.3: Second-order low pass filter	40
Fig. 4.4: Common LNA architectures, (a) Single-ended architecture and (b) Differential Architecture	42
Fig. 4.5: Miller effect of cascode stage	44
Fig. 4.6: Inductor $\pi$ -model	46
Fig. 4.7: Design procedure of Ultra-wide bandwidth (UWB) low noise amplifier (LNA)	48
Fig. 5.1: Simplified circuit of wideband LNA design	50
Fig. 5.2: Simplified small signal model at the input LNA stage	51
Fig. 5.3: Input network looking into cascode LNA	52
Fig. 5.4: Simplified LNA with bond wire effects take into consideration	53
Fig. 5.5: Input network of cascode LNA and bond wire effects.	54
Fig. 5.6: Equivalent model of low pass filter	56
Fig. 5.7: Summary of filter transformation	56
Fig. 5.8: Transformation of a low pass filter to band pass filter	57
Fig. 5.9: Sixth-order band pass filter for impedance matching	57
Fig.5.10: Simulated power gain without shunt peaking.	60
Fig.5.11: High frequency analysis, (a) Large signal high frequency model and (b) Small signal equivalent model for calculation.	61
Fig.5.12: DC supply biasing through second section of band pass filter signal equivalent model for calculation.	66
Fig.5.13: Cascode current mirror biasing	67
Fig. 6.1 : Ideal simulation implementation using ideal inductor	69
Fig. 6.2 : Actual simulation implementation using SIL18RF inductor	70
Fig. 6.3 : Actual simulation implementation using ASITIC inductor	71
Fig. 6.4 : Simple current mirror biasing	74
Fig. 6.5 : DC source biasing through LC filter	74
Fig. 6.6 : Cascode current mirror biasing	75
Fig. 6.7 : Temperature sensitivity on DC current biased by simple current mirror	77
Fig. 6.8 : Temperature sensitivity on DC current biased by DC source	78
Fig. 6.9 : Temperature sensitivity on DC current biased by cascode current mirror	78
Fig. 6.10: Input matching network and output matching network in circuit	80
Fig. 6.11: Simulated input reflection coefficient, $S_{11}$ for Ideal inductors	81
Fig. 6.12: Simulated output reflection coefficient, $S_{22}$ for Ideal inductors	82
Fig. 6.13: Simulated Reverse Isolation coefficient, $S_{12}$ for Ideal inductors	83

Fig. 6.14: Simulated Forward Transmission Gain, $S_{21}$ for Ideal inductors	84
Fig. 6.15: Simulated Noise Figure (NF) for Ideal inductors	85
Fig.6.16: Simulated Noise Figure Minimum ( $NF_{min}$ ) for Ideal inductors	86
Fig.6.17: Simulated input reflection coefficient, $S_{11}$ for three sub-bands	88
Fig.6.18: Simulated Reverse Isolation coefficient, $S_{12}$ for three sub-bands	89
Fig.6.19: Simulated Forward Transmission Gain, $S_{21}$ for three sub-bands	89
Fig.6.20: Simulated Output reflection coefficient, $S_{22}$ for three sub-bands	90
Fig.6.21: Simulated Noise Figure, NF for three sub-bands	90
Fig.6.22: Simulated Noise Figure Minimum, $NF_{min}$ for three sub-bands	91
Fig.6.23: Simulated input reflection coefficient, $S_{11}$ for original ASITIC	92
Fig.6.24: Simulated output reflection coefficient, $S_{22}$ for original ASITIC	93
Fig.6.25: Simulated reverse isolation coefficient, $S_{12}$ for original ASITIC	93
Fig.6.26: Simulated forward transmission gain, $S_{21}$ for original ASITIC	94
Fig.6.27: Simulated noise figure, NF for original ASITIC	94
Fig.6.28: Simulated noise figure minimum, $NF_{min}$ for original ASITIC	95
Fig.6.29: Simulated input reflection coefficient, $S_{11}$ for ASITIC and SIL18RF	98
Fig.6.30: Simulated Output reflection coefficient, $S_{22}$ for ASITIC and SIL18RF	98
Fig.6.31: Simulated Reverse Isolation coefficient, $S_{12}$ for ASITIC and SIL18RF	99
Fig.6.32: Simulated Forward Transmission Gain, $S_{21}$ for ASITIC and SIL18RF	99
Fig.6.33: Simulated Noise Figure, NF for ASITIC and SIL18RF	100
Fig.6.34: Simulated Noise Figure Minimum, $NF_{min}$ for ASITIC and SIL18RF	100
Fig.6.35: Simulated input reflection coefficient, $S_{11}$ for Ideal and ASITIC	101
Fig.6.36: Simulated Output reflection coefficient, $S_{22}$ for Ideal and ASITIC	102
Fig.6.37: Simulated Reverse Isolation coefficient, $S_{12}$ for Ideal and ASITIC	102
Fig.6.38: Simulated Forward Transmission Gain, $S_{21}$ for Ideal and ASITIC	103
Fig.6.39: Simulated Noise Figure, NF for Ideal and ASITIC	103
Fig.6.40: Simulated Noise Figure Minimum, $NF_{min}$ for Ideal and ASITIC	104
Fig.6.41: Simulated Input referred 1dB Compression for simple current mirror	106
Fig.6.42: Simulated Input referred 1dB Compression for DC source	107
Fig.6.43: Simulated Input referred 1dB Compression for cascode current mirror	107
Fig.6.44: Simulated Output referred 1dB Compression for simple current mirror	108
Fig.6.45: Simulated Output referred 1dB Compression for DC source	108
Fig.6.46: Simulated Output referred 1dB Compression for cascode current mirror	109
Fig.6.47: Simulated Input referred 1dB Compression for 3.432GHz	110
Fig.6.48: Simulated Output referred 1dB Compression for 3.432GHz	111
Fig.6.49: Simulated Input referred 1dB Compression for 4.488GHz	111
Fig.6.50: Simulated Output referred 1dB Compression for 4.488GHz	112
Fig.6.51: Simulated Input referred 1dB Compression for SIL18RF	113
Fig.6.52: Simulated Output referred 1dB Compression for SIL18RF	114
Fig.6.53: Simulated Input referred 1dB Compression for ASITIC	114
Fig.6.54: Simulated Output referred 1dB Compression for ASITIC	115
Fig.6.55: Simulated Input Third Order Intercept Point (IIP3) for ideal simulation	116
Fig.6.56: Simulated Output Third Order Intercept Point (OIP3) for ideal simulation	117
Fig.6.57: Simulated Input Third Order Intercept Point (IIP3) for ASITIC simulation	117
Fig.6.58: Simulated Output Third Order Intercept Point (OIP3) for ASITIC simulation	118
Fig. 7.1 : Distributed resistance in diffusion area	123
Fig. 7.2 : Design Flow in Layout for this project	124
Fig. 7.3 : Layout of ASITIC inductor	126

Fig. 7.4 : Layout of Poly Silicon Pattern Ground Shield	126
Fig. 7.5 : Layout of bonding pad	127
Fig. 7.6 : Layout of LNA with SIL18RF inductor	129
Fig. 7.8 : Layout of ASITIC LNA	130
Fig. 8.1 : Pin configuration of MAX2654	133
Fig. 8.2 : Typical operating circuit for MAX2654	133
Fig. 8.3 : MAX 2654 Evaluation kit circuit	134
Fig. 8.4: Photo on MAX 2654 Evaluation kit	135
Fig. 8.5: The network analyzer	137
Fig. 8.6: Setup for measuring the scattering parameter using Network analyzer, HP8753E	138
Fig. 8.7 : Spectrum analyzer HP 8593E	139
Fig. 8.8 : RF signal generator, HP 8648B	140
Fig. 8.9 : The setup of spectrum analyzer and signal generator.	141
Fig.8.10: Graph shows supply current versus supply voltage	143
Fig.8.11: Measurement of Input Return Loss ( $S_{11}$ ) in MAX 2654.	144
Fig.8.12: Measurement of Output Return Loss ( $S_{22}$ ) in MAX 2654.	144
Fig.8.13: Measurement of Reverse Isolation ( $S_{12}$ ) in MAX 2654.	145
Fig.8.14: Measurement of Forward Transmission Gain ( $S_{21}$ ) in MAX 2654.	145
Fig.8.15: Measurement of Input Return Loss, $S_{11}$ (dB) over Supply voltage (V)	147
Fig.8.16: Measurement of Reverse Isolation, $S_{12}$ (dB) over supply voltage (V)	147
Fig.8.17: Measurement of forward transmission gain, $S_{21}$ (dB) over Supply Voltage (V)	148
Fig.8.18: Measurement of Output Return Loss, $S_{22}$ (dB) over supply voltage (V)	148
Fig.8.19: Measurement of 1dB compression point	150
Fig.8.20: Measurement of Output power over supply voltage (V)	150
Fig.8.21: Test circuit setup for chip characterization	152

## LIST OF TABLES

	<b>PAGE</b>
Table 1.1 : Characteristic of UWB Technology	3
Table 1.2 : The Goal of Proposed Low Noise Amplifier	5
Table 2.1 : Classification of Signals based on Fractional Bandwidth	9
Table 2.1 : Link Budget of Mode 1 OFDM	14
Table 3.1 : Comparison between Direct Conversion (DICON) and Superheterodyne of UWB Receiver Architectures	28
Table 5.1 : Element values of equal ripple Low Pass Filter with 0.1dB ripple	55
Table 5.2: Summary of new element values of transformed band pass filter	58
Table 5.3: Summary of Input Network element values	59
Table 5.4: Capacitance obtained from Cadence's Result Browser	61
Table 5.5 : Current budget for each Major Block in LNA design	65
Table 6.1 : Physical Elements of Equivalent pi-model of ASITIC Inductor	72
Table 6.2 :Comparison on Width of Each Transistor Obtained from Simulation	73
Table 6.3 : Temperature Sensitivity on DC Current	76
Table 6.4 : Current Budget of Each Stage in LNA Design	79
Table 6.5 : Power Consumption of Each Stage in LNA Design	79
Table 6.6 : Comparison on SP Analysis among Three Biasing Techniques	86
Table 6.7 : Comparison on S-Parameter analysis for Three Sub-bands	88
Table 6.8 : A Summary of ASITIC Performance without Pattern Ground Shield	92
Table 6.9 : Physical Elements of Generated ASITIC Inductor after Tuning	96
Table6.10: Comparison between ASITIC and SIL18RF from SP Analysis	97
Table6.11: Comparison on 1dB Compression Point for Input and Output Power among Three Biasing Techniques	106
Table6.12: Comparison on 1dB Compression Point for Input and Output Power among Three Sub-bands	109
Table6.13: Comparison of PSS Analysis for ASITIC and SIL18RF	113
Table6.14: Comparison between Measured Specifications and Simulation Results	120
Table6.15: Comparison between Ideal model and Actual model in Input Matching Network	121
Table6.16: Comparison between Ideal model and Actual model Output Matching Network	121
Table 8.1 : Pin Description of MAX 2654 EV kit	133
Table 8.2 : Description of Test Equipments	135
Table 8.3 : SPECIFICATIONS OF MAX2654	136
Table 8.4 : The Measurement of DC Biasing	142
Table 8.5 : Comparison between Specifications and Measurement Results	146
Table 8.6 : Measurements of S-Parameter with respect to various Supply Voltages	146
Table 8.7 : Measurement data of Output Power due to various Supply Voltages and Input Power	149
Table 9.1 : A Comparison with Work Done by Others	156

## CHAPTER 1

### INTRODUCTION

#### 1.1 Introduction to Ultra-Wide Bandwidth (UWB) Technology

During the last decade, wireless communication technology has undergone a rapid commercial development. Due to the fact that current narrow-band and wideband technologies cannot satisfy the improvement of wireless technology, new enhanced technology for higher capacity, faster services and more secure wireless connections will be necessary, namely Ultra-wideband (UWB) technology.

UWB is a low power technology that can support very high data rates over a short range for personal connectivity. As such, this technology brings the convenience and mobility of wireless communications to high-speed interconnects in devices through the homes and offices. UWB is the leading technology for freeing people from wired world and brings us one-step closer to wireless freedom. In other words, UWB technology is complementary to IEEE 802.11 WLAN (Wireless Local Area Network) which is best suited for long-range networking and Ethernet cable replacement.

On 14 February 2002, the Federal Communication Commission (FCC) in United States has approved the use of Ultra-wideband (UWB) technology for commercial applications. UWB technology has a broader spectrum that is ranging from 3.1 GHz to 10.6 GHz (low frequency band: 3.1 GHz to 5 GHz; high frequency band: 6 GHz -10.6 GHz). As defined by the FCC's Final Report and Order, UWB signals must have bandwidths of greater than 500 MHz or a fractional bandwidth larger than 25 percent. Hence, for multi-band approach, the entire frequency spectrum of UWB divides into multiple smaller bandwidths with bandwidth of 528 MHz. The low frequency band, which consists of the first three sub-bands allocated for the first generation UWB system, called UWB mode 1 application.

UWB is capable of supporting high data rates within a short range, while the pricing is low and embedded with low power technology. Two recent proposals for the

IEEE 802.15.3a proposed that data rates of up to 400-480 Mbps at a distance of 2m and 110 Mbps at a distance of 10m. High data rates due to larger bandwidths for UWB pulses.

UWB technology is a low power technology as it is allowed to operate at a maximum power spectral density  $-41 \text{ dBm / MHz}$  (or  $79 \text{ nW / MHz}$ ). Hence, it is categorized as unintentional radiators such as TVs and computer monitors. This power restriction allows UWB system to reside below the noise floor of a typical narrow band receiver. Moreover, the power requirement enables UWB signals to coexist with current radio services with minimal or no interference [Leenaerts and Bergervoet, 2005].

Moreover, low power consumption makes it feasible to develop cost effective CMOS implementation. The ever continuing downscaling of CMOS technologies has resulted in full integration between analog RF block and Digital Signal Processing (DSP) block, which constitutes System-On-Chip (SOC). In low noise RF circuits, accurate modeling of noise in CMOS technologies is a prerequisite [Belk, 2004].

For mode 1 application, it consists of three sub-bands of lower frequency spectrum of UWB. Every sub-band has a bandwidth of 528 MHz with a carrier center frequency such as 3.432 GHz (first sub-band), 3.96 GHz (second sub-band), and 4.488 GHz (third sub-band). Fig. 1.1 shows the band plan of these three sub-bands. Quadrature Phase-Shift-Keying (QPSK) was implemented in this design. Information data rates of UWB mode 1 application can achieve up to 480 Mbps at a distance of 2m, 200 Mbps a distance of 4 m as well as 110 Mbps at a distance of 10m. Due to Mode 1 the bandwidth of 528 MHz on each sub-band for Mode 1 radio, only a fraction of time is transmitted because of time-division multiplexing. Hence, the average transmitter power is shown as  $-10.3 \text{ dBm}$  for three information data rates. Transmit power is calculated by multiplying the allowed limit of power level in UWB transmission,  $-41 \text{ dBm / MHz}$  by the bandwidth of the signal. On the other hand, average of received power shows a maximum of  $-60.5 \text{ dBm}$  at 480 Mbps and a minimum of  $-74.5 \text{ dBm}$  at 110 Mbps. Summary characteristic of mode 1 of UWB technology is shown as in Table 1.1.

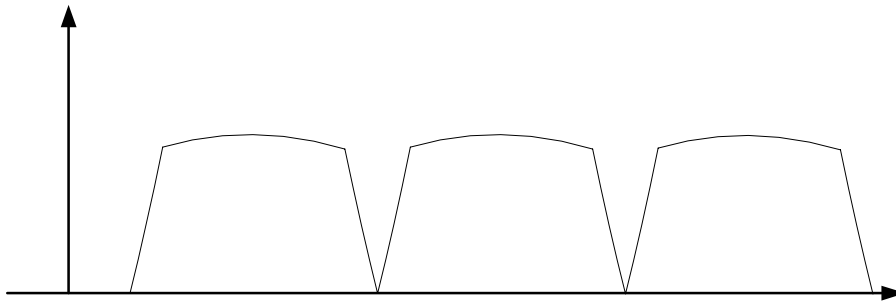


**Fig 1.1** Band plan in Mode 1 UWB application

**Table 1.1** Characteristic of UWB Technology

Carrier Centre Frequency	3.432GHz, 3.96GHz, 4.488GHz
Channel Bandwidth	528MHz for each sub-band
Modulation	QPSK
Operating range	10m, 4m ,2m
Transmitted power	-10.3 dBm
Received power	-60.5 dBm (10m), -66.5 dBm (4m) and -74.5 dBm (2m)
Information data rate	110Mbps, 200Mbps, 480Mbps

## 1.2 Objective

The objective of this project is to design a UWB low-noise amplifier, which is capable of transmitting data over a wide spectrum of frequency bands under very low power consumption and high data rates. As compared to conventional technology, UWB technology offers promising solutions to the RF spectrum by allowing new services to exist with current radio systems with minimal or no interference. Among the possible applications, UWB technology may be used for imaging systems, vehicular and ground-penetrating radars, and communication systems. In particular, it is envisioned to replace almost every cable at home or in an office with a wireless connection that features hundreds of megabits of data per second [Bevilacqua and Niknejad, 2004].

For this project, a wideband LNA operating over the entire 1.8 GHz (3.1GHz-4.9GHz) band of operation is required. The designed low noise amplifier

based on the previous work presented by Bevilacqua and Niknejad. The function of a low noise amplifier has to take charge of amplification of RF signal while producing as little noise as possible in order to fall in desired dynamic range. For UWB application, such an amplifier must feature a wideband input matching to a  $50\Omega$  antenna for noise optimization as well as filtering out-of-band interferers. Moreover, it must show flat gain over the entire bandwidth, good linearity, a minimum possible noise figure (NF) and low power consumption.

The LNA was implemented for UWB mode 1 application, which is covering the frequency spectrum from 3.1 GHz to 4.9 GHz. Good matching at the input and output port ensure minimum reflection from both ports; hence, alleviate signal loss problem in LNA. The input and output matching are measured by input reflection coefficient,  $S_{11}$  and output reflection coefficient,  $S_{22}$ . Both parameters should exhibit values below -10 dB in order to have minimum reflection from the port. High gain larger than 9.3 dB [Bevilacqua and Niknejad, 2004] and gain flatness within  $\pm 1$  dB are the goals in design performance. In terms of low noise in LNA, noise figure, NF and noise figure minimum,  $NF_{\min}$  is targeted to be less than 4 dB [Bevilacqua and Niknejad, 2004]. Linearity of LNA is also crucial, as it must remain linear for the entire dynamic range. Hence, 1 dB compression point ( $P_{1dB}$ ) and third order intercept point (IIP3) are needed to measure the linearity of LNA in order to fall in desired goals. Moreover, low power consumption which is less than 18 mW [Bevilacqua and Niknejad, 2004] to achieve low power application. Area of less than 2 mm x 2 mm is needed to fulfill the Silterra requirement in chip fabrication. The goals of the proposed amplifier are summarized in Table 1.2.

### 1.3 Design Flow

Fig. 1.2 represents the design flow of this project. There are two phases: design simulation and hardware measurement on MAX 2654 evaluation kit. In phase 1, four stages are involved; schematic entry, circuit optimization, circuit verification and chip fabrication. Optimization is crucial in the second stage in order to obtain optimum

**Table 1.2:** The Goals of Proposed Low Noise Amplifier

Parameters	Specifications
Bandwidth, B	3.1 GHz-4.9 GHz
Input / Output matching, $S_{11}$ and $S_{22}$	<-10 dB
Power gain, G	>9.3 dB
Noise figure, NF	<4 dB
Noise figure minimum, $NF_{min}$	<4 dB
1dB Compression Point, $P_{1dB}$	-16.7 dBm
Supply voltage, $V_{dd}$	1.8V
Power Consumption, $P_{dc}$	<18 mW
Chip area size, A	2 mm x 2 mm

performance before proceeding to physical implementation. The circuit is verified using tools of Design Rule Check (DRC) and Layout Versus Schematic (LVS). DRC checks on the connectivity error in the schematics while LVS is a comparison check on mismatches between schematic and layout. Finally, design is sent to Silterra for chip fabrication.

In second phase, measurements are carried out using purchased evaluation kit. In this phase, measurement tools such as spectrum analyzer, network analyzer, and signal generator are used to measure AC characteristics as well as DC characteristics of the evaluation kit. Furthermore, a printed circuit board (PCB) using Duroid is constructed for future characterization on fabricated chip.

#### 1.4 Project Overview

The purpose of this dissertation is to present the LNA design applicable to new enhance technology, UWB technology. It begins with an introduction, overview of the project as well as objectives of this project. The ultimate goal for this work is to design the front-end UWB LNA in 0.18 $\mu$ m Silterra CMOS process.

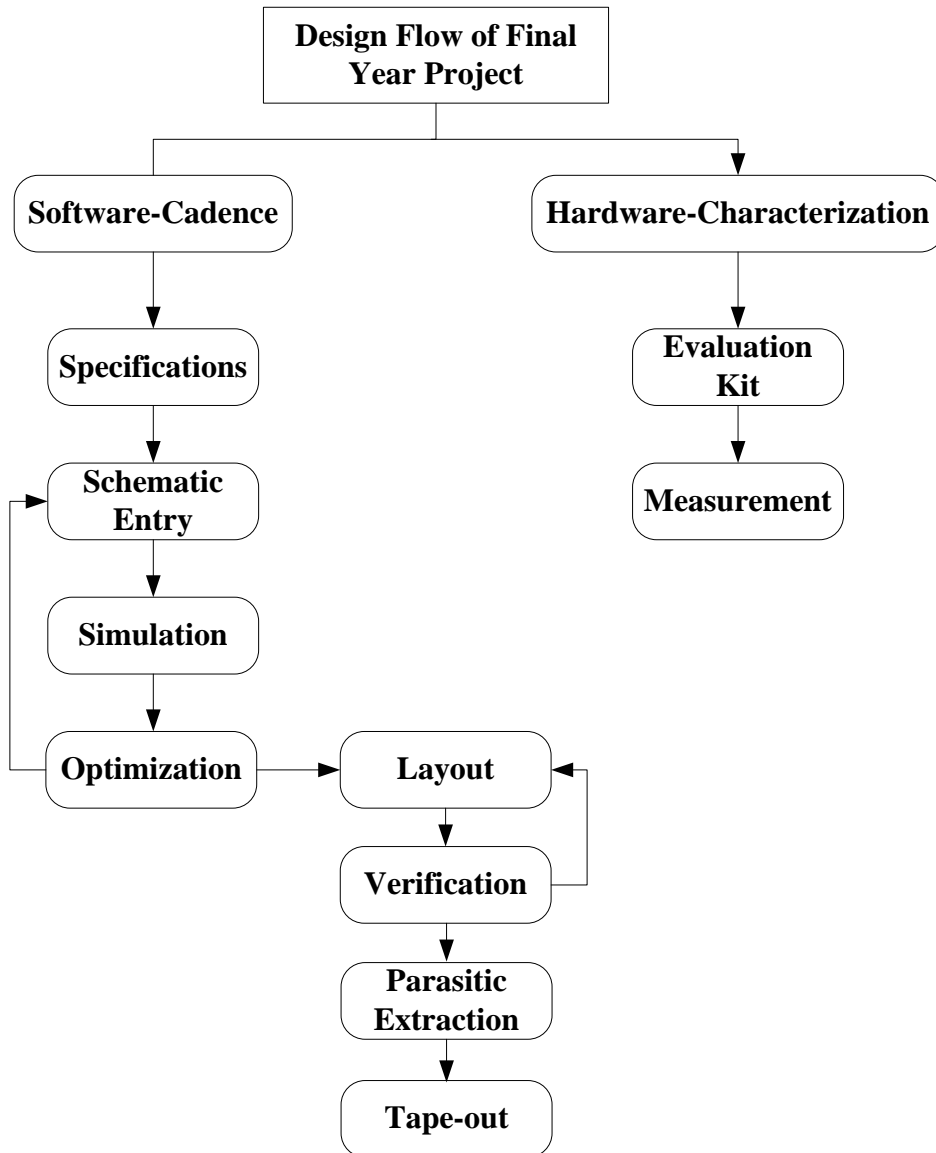


**Fig. 1.2** Typical design flow of final year project

Chapter 2 covers an overview of UWB system as well as modulation scheme of multi-band approach employed in the system. Comparison between single band approach and multi-band approach is presented too. Finally, it ends with an overview of RF circuit design fundamentals. The fundamentals include impedance matching issues and linearity issues of the LNA.

Chapter 3 discusses on the requirements of UWB receiver by looking into various existing receiver architectures. Besides, an overview on roles of each RF components in the receiver is also presented. Chapter 4 reviews the current advances of

LNA from technological and architectural points of view. The existing topologies of LNA is being studied and compared. Overview on passive elements employed in this design is also included. Finally, it ends with design procedure of the LNA.

In Chapter 5, the circuit analysis on LNA design section discusses on the input impedance, wideband impedance matching, and gain enhancement technique as well as noise analysis on LNA. Besides, additional biasing circuitry such as simple current mirror biasing, DC biasing and cascode current mirror biasing are also included in this section.

Discussions on the simulation results are presented in Chapter 6 in terms of comparison between ideal simulation and actual simulation. Ideal simulation is due to the usage of ideal inductor from analog library, whereas, actual simulation is due to actual inductor generated using ASITIC or inductors from SIL18RF library.

Chapter 7 provides the layout guidelines and discusses verification on the physical implementation. Hardware measurement on MAX 2654 evaluation kit is presented in Chapter 8. This section presents calibration steps uses in the measurement and its setup. It ends with summary, discussions and comparison between specifications of the kit versus measurement results.

Finally, conclusions and suggestions are included in order to improve the performance of designed low noise amplifier for future work.

**CHAPTER 2****BASIC AND RF FUNDAMENTALS OF  
ULTRA-WIDE BANDWIDTH (UWB) SYSTEM**

Ultra-wideband (UWB) technology brings the convenience and mobility of wireless communications to high-speed interconnects in devices such as Universal Serial Bus (USB) throughout the digital home and office. It frees people from wired world to wireless freedom and enables consumers to access a wide range information from anywhere at any time. It is the leading wireless personal area networks (WPAN) technology, which has frequency spectrum ranging from 3.1 GHz to 10.6 GHz.

IEEE 802.15.3a is a task group (TG3a) for Wireless Personal Area Network (WPAN). The purpose of this task group is to provide a specification for a low complexity, low cost and low power consumption, as well as high data rates of wireless connectivity among devices within or entering the Personal Operating Space [Ryan et al, 2004].

In this section, the understanding of UWB signal employing in UWB system, approach of UWB as well as link budget of Multi-band OFDM Approach (MBOA) UWB system are presented. Understanding on UWB signal in UWB technology is highlighted as it is much different from conventional technology.

In RF system, matching and linearity are the basic specifications of system performance. Impedance matching is the major contributor to gain efficiency as well as noise optimization. On the other hand, linearity limits the system dynamic range and signal distortion. These important considerations are also included in this section.

**2.1 UWB Technology**

A successful radio system design requires the understanding of the characteristics of the signal that drives the system. Since this UWB radio is much different from conventional radio system, understanding of these signal characteristics

is very important.

Traditional narrow band communication systems require a specific carrier frequency to transmit and receive information. By having signal energy in a narrow frequency spectrum, it is vulnerable to interference. Unlike narrow band systems, UWB systems use carrier-less transmission in short duration (picoseconds to nanoseconds) UWB pulses with low duty cycle. Low duty cycle directly translates to longer battery life for handheld equipment. As frequency inversely related to time, the short duration of UWB pulses can be represented by a spread spectrum across a wide range of frequencies. Consequently, UWB signals have wider bandwidths.

Hence, bandwidth is perhaps the most important characteristic of UWB communication systems. As defined by Federal Communication Commission (FCC), UWB signals must have bandwidths of greater than 500 MHz or fractional bandwidth larger than 25 percent. Fractional bandwidth is a factor used to classify signal as narrow-band, wideband, or ultra-wideband. It represents the ratio of bandwidth at -10 dB to centre frequency. Fractional bandwidth of less than 1 percent indicates a narrow-band signal while wideband signal is shown in Table 2.1 [Barras et al, 2002].

**Table 2.1** Classification of Signals based on Fractional Bandwidth

Signals	Fractional bandwidth, $B_f$ (%)
Narrow-band	$B_f < 1 \%$
Wideband	$1 \% < B_f < 20 \%$
Ultra-wideband	$B_f > 25 \%$

One of the major advantages of the large bandwidth for UWB pulses is improved data rate. Data rate, or channel capacity, is defined as the maximum amount of data that can be transmitted per second over a communication channel [Tomasi, 2004]. The large channel capacity of UWB communications systems is evident from Shannon's capacity theorem [Tomasi, 2004] as

$$C = B \log_2(1 + SNR) \quad (2.1)$$

where  $C$  represents maximum channel capacity,  $B$  is the bandwidth and SNR is signal-to-noise power ratio. It shows that channel capacity is proportional to bandwidth of a channel. Hence, having large bandwidth of 7.5 GHz (3.1 GHz to 10.6 GHz), high data rates can be expected. IEEE 802.15.3a is the IEEE standard that will define an alternative physical layer (PHY), based on UWB, that will provide in excess of 110 Mbps at a 10m distance and 480 Mbps at 2m [Ryan et al, 2004].

On the other hand, as mentioned before, UWB technology is a promising technology that allows UWB signal to coexist with current radio services with minimal or no interference. This has solved problems of overcrowded in RF spectrum by using conventional technology. Secure communications offered by UWB signal make UWB technology become attractive among consumers. Due to low transmission power and short UWB pulses, which is picoseconds pulses, the probability of transmitted information to be detected in these communication systems is low. Therefore, UWB systems hold significant promise of achieving high security, low probability of interference communications.

Apart from high data rates, secure communication and increase the application in WPAN, UWB technology offers low power and low cost application as well as better material penetration as compared to conventional technology. The FCC power requirement of -41.3 dBm / MHz, which is 79 nW / MHz for UWB systems, puts them in the category of unintentional radiators such as monitors and computers. Such power limitation in transmission makes it ideal for short-range use, specifically for WPAN. Low power characteristic of UWB technology make it feasible for CMOS implementation, leading to low cost production [Batra et al, 2003].

Unlike narrow-band technology, UWB systems can penetrate effectively through different materials. However, it is only useful when they are allowed to occupy low-frequency portion of the radio spectrum. Moreover, carrier-less transmission of UWB pulses require fewer RF components in system implementation than carrier-based transmission. Since it is carrier-less, there is no need for carrier recovery stage at the receiving end. In general, the analog front-end of UWB transceiver is less complicated

than a narrowband transceiver.

In summary, UWB systems are a new wireless technology capable of transmitting data over a wide spectrum of frequency bands with very low power and high data rates. Among the possible applications, UWB technology may be used for imaging system, vehicular and ground-penetrating radars, and communication systems [Bevilacqua and Niknejad, 2004].

## **2.2 Approach of UWB System**

UWB systems can be categorized into two types: conventional UWB systems and modern UWB systems. A conventional system is also referred as single band approach, which is original UWB approach using narrow pulses that occupy a large portion of spectrum at several GHz in a bandwidth. The corresponding receiver then translates the pulses into data by listening for a familiar pulse sequence sent by the transmitter. In other words, single band approach utilizes a single carrier in the transmission.

Apart from the conventional way, modern UWB system uses multiple bands approach for data transmission. Multi-band approach divides the available UWB frequency spectrum into several multiple and non-overlapping bands with bandwidths greater 500 MHz to achieve FCC definition of UWB signal. By using multi band approach, efficiency of the system can be achieved as UWB spectrum has been utilized by transmitting multiple UWB signals at the same time. The signals will not interfere with each other because they operate at different frequencies within the spectrum. It offers capability to avoid potential interference as transmission over certain bands can be avoided. Besides that, smaller bandwidths can be used to process the information. Thus, the complexity of the design is reduced, as well as the cost and power consumption of the system.

### **2.2.1 Multi-band Approach**

At present, there are two separate architectures for UWB modulating

technologies under consideration from IEEE 802.15.3a. These two techniques of implementing multi band UWB are Direct Sequence Code Division Multiple Access (DS-CDMA) and Pulsed Orthogonal Frequency Division Multiple Access (OFDM) [Ryan et al, 2004].

DS-CDMA is powerful multiple access technique in the presence of strong narrow band interference as well as bandwidth efficiency for multi-user wireless communication. However, the feature of overcoming the interference lies in its advanced receiver that can incorporate various levels of DSP to increase their performance while power and cost of the receiver increases accordingly [Ryan et al, 2004].

OFDM is another spread spectrum technique, which distributes data over a large number of carriers that are spaced apart at precise frequencies. Hence, OFDM is multi-carrier modulation scheme and information is being transmitted on each of the sub-bands. OFDM has several good properties, including high spectral efficiency, inherent resilience to RF interference, robustness to multi-path, and the ability to capture multi-path energy efficiently. It is also well understood and has been proven in other commercial technologies (ex. IEEE 802.11a/g). Band plan of OFDM is shown in Fig. 2.1. In order to achieve FCC definition of UWB signal, bandwidth occupies in each sub-band must be greater than 500 MHz. Therefore, 528 MHz is chosen.

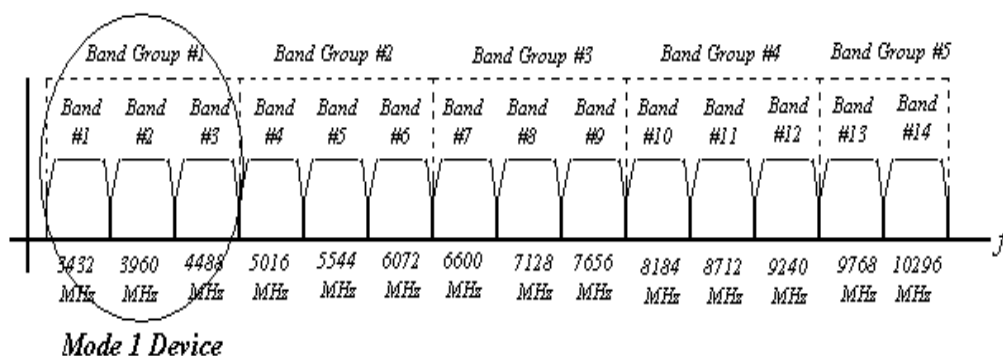


**Fig. 2.1:** Band plan of multi band OFDM. The center frequency is shown at the bottom of each band.

For this project work, only mode 1 of UWB is implemented for the design of low-noise amplifier. Mode 1 consists of three sub-bands, which has the frequency ranging from 3.1 GHz to 4.9 GHz. Table 2.2 shows link budget of Multi-band OFDM Approach (MBOA) specifications. It is a link budget that indicates the critical top-level requirements for the system including transmit power, path loss, required sensitivity and link margin. The table has three columns, each associated with a different data rate and range. The third column presents the highest data rate of 480 Mbps and the associated range of only two meter, whereas, the first column indicates the lowest data rate of 110 Mbps and associated range of only 10 meters.

The transmit power is calculated based on FCC part 15 regulation. The transmit power is calculated by multiplying the allowed limit of power level in UWB transmission, -41dBm / MHz by the bandwidth of the signal. The biggest loss in the system is path loss. Batra et. al give the path loss of a radio channel as the following [Batra et. al, 2003]:

$$Path\ Loss(dB) = 20\log\left(\frac{c}{4\pi rf}\right) \quad (2.2)$$

Where  $f$  is the geometric centre frequency,  $r$  is the range of transmission, and  $c$  is the speed of light in free space,  $3 \times 10^8 \text{ ms}^{-1}$ . A link budget generally depicts values for a single frequency. For UWB, some frequency is needed in order to compute the path loss. The generally accepted method to calculate the frequency,  $F_c$  is to select the geometric mean of the high frequency,  $F_{high}$  and low frequency,  $F_{low}$  [Batra et al, 2003]:

$$F_c = \sqrt{F_{low} \cdot F_{high}} \quad (2.3)$$

Receiver sensitivity of different data rates is also included in the table. It is defined as the minimum signal threshold that can be detected in the presence of noise. For QPSK modulation and a Bit Error Rate (BER) of  $1\text{E}^{-10}$ , the required signal-to-noise ratio for an acceptable bit error rate,  $E_b / N_0$  is 4.0 dB. CMOS receiver noise figure (NF) of 6.6 dB was selected as typical value, which is achievable for CMOS implementation. The implementation loss is also included in the system that can add to the noise, the sensitivity can be adjusted by adding an additional 2.5 dB in order to obtain the receiver

sensitivity of -80.5 dBm for data rates of 110 Mbps.

Link margin is a calculation of the additional power over and above the minimum detectable level. It provides some headroom for design modifications and any tolerances exist in the transceiver design. System margin avoids us to operate the system in at the limits of sensitivity [Batra et al, 2003]. [Williams et al, 2005] gives the system margin as:

$$\text{Margin} = \text{Received Power} - \text{Sensitivity} \quad (2.4)$$

**Table 2.2:** Link Budget of Mode 1 OFDM [Batra et al, 2003]

Parameter	Value	Value	Value
Information Data Rate	110 Mbps	200 Mbps	480 Mbps
Distance	10 m	4 m	2 m
Average Tx Power	-10.3 dBm	-10.3 dBm	-10.3 dBm
Total Path Loss	-64.2 dB	-56.2 dB	-50.2 dB
Geometric Centre Frequency	3883 GHz	3883 GHz	3883 GHz
CMOS Rx Noise Figure	6.6 dB	6.6 dB	6.6 dB
Required $E_b/N_0$	4.0 dB	4.7 dB	4.9 dB
Implementation Loss	2.5 dB	2.5 dB	3.0 dB
Rx Sensitivity Level	-80.5 dBm	-77.2 dBm	-72.7 dBm
Link Margin	6.0 dB	10.7 dB	12.2 dB

## 2.3 RF Fundamentals

In any RF system, matching and linearity are the two basic specifications of system performance. Impedance matching is the major contributor to gain efficiency. Whereas, linearity limits the system's working range.

### 2.3.1 Impedance Matching

Impedance matching is often a part of the larger design process for a microwave component or system. The basic idea is illustrated in Figure 2.2, which

shows an impedance matching network placed between load impedance and a transmission line. The matching network is assumed to be lossless, the characteristic impedance,  $Z_0$  with equals to  $50 \Omega$ . Then the reflection is eliminated on the transmission line to the left of the matching network, although there will be multiple reflections between the matching network and the load [Pozar, 1998].



**Fig. 2.2:** A lossless-matching network

To achieve maximum power transfer, impedance matching between the load and the source is the essential requirement. Usually, passive networks connected between the source and the load used to accomplish this matching. This matching network is designed not only to achieve minimum power loss between the load and the source, but also to minimize noise, to maximize power handling capability and to obtain desired frequency response.

Impedance matching is very important for several reasons. Firstly, maximum power is delivered when the load is matched to the line while power loss is minimized in the feed line. Despite that, there are some impedance matching sensitive receiver components available such as antenna, low-noise amplifier, etc. Thus, improving the impedance matching for these receiver components will therefore improve the signal-to-noise ratio of the system. Impedance matching in a power distribution network such as antenna array feed network will reduce amplitude and phase errors.

As with most engineering solutions, the simplest design that satisfies the required specifications is generally the most preferable. A simple matching is usually cheaper, more reliable, and less lossy than a more complex design. On the other hand, any type of matching network can ideally give a perfect match that is zero reflection at a single frequency. In UWB applications, however, it is desirable to match a load over a

band of frequencies. There are several methods in doing this at the expense of complexity. Furthermore, it also depends on the type of transmission line being used. In some applications, adjustment to matching network is required in order to match variable load impedance. Some types of matching networks are more amenable than others in this regard [Pozar, 2001].

### 2.3.2 Linearity

In addition to input match, signal distortion and dynamic range are other important consideration because LNA must do more than simply amplify signals without adding much noise. It must also remain linear even when strong signals are being received. In particular, the LNA must maintain linear operation when receiving a weak signal in the presence of a strong interfering one. These consequences of inter-modulation distortion include desensitization (also known as blocking) and cross modulation. Blocking occurs when the inter-modulation products caused by the strong interferer swamp out the desired weak signal, whereas cross-modulation results when nonlinear interaction transfers the modulation of one signal to the carrier of another. Both effects are clearly undesirable; therefore, another function of an LNA is to mitigate these problems to the maximum practical extent [Lee, 2002].

Although most of the system design uses a linear approximation, signal distortion makes it not valid in its non-linear region. The distorted signal might have lost some critical information need at the receiving end. This signal distortion can be specified by 1 dB compression point and third order intercept point (IP3) that will be described in the subsequent section. These definitions are two different ways to describe system's linearity.

#### 2.3.2.1 1-dB Compression Point ( $P_{1dB}$ )

As the input signal approaches to the system's saturation region, the system signal gain begins to fall off. The point where the gain of the system deviates from its linear approximation by 1 dB is called the 1 dB compression point. This 1dB compression

point can be used to be defined the extent of the linear region. Therefore, the system's dynamic range can be defined as the power difference from the noise level to the 1 dB compression point. Figure 2.3 shows how the dynamic range is set from the relationship between input and output power. It is shown that the nonlinearity sets the maximum signal level of the system,  $P_{out, 1dB}$  while the minimum output power level where the input power referred as  $P_{in, MDS}$  is indicated as  $P_{out, MDS}$ . Hence, the dynamic range,  $d_R$  is the difference between the maximum output power level and the minimum output power level without entering the nonlinearity region.

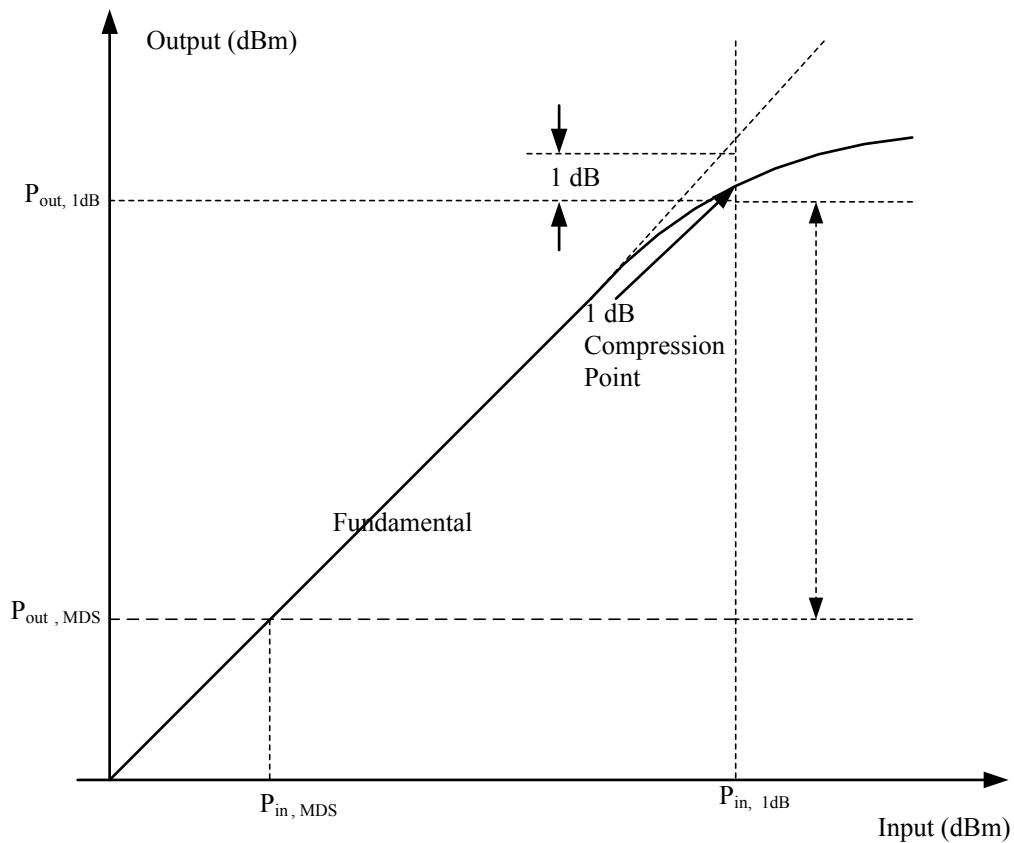


**Fig. 2.3:** The dynamic range of system from input and output power relation

### 2.3.2.2 Third Order Intercept (IP3)

In narrow-band circuits, distortion is commonly measured by applying two pure sinusoidal signals of slightly different frequencies ( $\approx$  MHz range) to the input of the system. These frequencies can be labeled as  $f_1$  and  $f_2$ . When two signals with different

frequencies are applied to a nonlinear system, the outputs exhibit some components that are not harmonics of the input frequencies such as distortion products that fall at the frequencies  $2f_1-f_2$ ,  $2f_2-f_1$ ,  $3f_1-f_2$ ,  $3f_2-2f_1$ , etc. As shown in Figure 2.4, these frequencies should be within the bandwidth of the circuit and thus can be used to measure the inter-modulation distortion, or IMD, produced by the circuit [Kundert, 2002].

For two sinusoidal input signals of equal amplitude,  $A$ , but slightly different frequencies at  $\omega_1$  and  $\omega_2$ , respectively given by

$$v = A[\cos(\omega_1 t) + \cos(\omega_2 t)] . \quad (2.5)$$

Then, the nonlinear system output comes as a power series of

$$V_{out} = a_1 V_{in} + a_2 V_{in}^2 + a_3 V_{in}^3 \quad (2.6)$$

where  $a_1$ ,  $a_2$  and  $a_3$  are gain of the input voltage,  $V_{in}$ . Expanding this output, results in several distortion products at frequencies at  $n\omega_1 \pm m\omega_2$  where  $n$  and  $m$  is the order of the distortion product. The amplitude of each product varies proportional  $A^{n+m}$ . Hence, the second order products vary in proportion to  $A^2$  while the third order products vary proportional to  $A^3$ . Noted that third order intermodulation distortion requires special attention as compared to second order distortion, which can be cancelled using differential implementation [Lee, 2002].

Fig. 2.4 shows that third order intercept point, IP3 by applying two equal amplitude sinusoidal signals, while increasing their power. The power at the output of fundamental (either  $f_1$  or  $f_2$ ) and  $n^{\text{th}}$  order inter-modulation product (for IP3 use either  $2f_1-f_2$  or  $2f_2-f_1$ ) are plotted. The  $n^{\text{th}}$  order intercept point IPn is defined in terms of the power levels of the power levels of the fundamentals and the  $n^{\text{th}}$  order products as extrapolated from their asymptotic small-signal behavior. When the input signal is small, a doubling of the input power doubles the fundamental output power and multiplies the output power of the  $n^{\text{th}}$  order products by  $2^n$ . Thus, the asymptotic slope of the fundamentals is 1dB/dB and the asymptotic slope of the  $n^{\text{th}}$  order product is  $n$  dB/dB. Since third order products grow as the cube of the amplitude, it exhibits a slope that is three times that of the fundamental output when plotted on logarithmic scales, as in Fig,

2.4 [Lee, 2002].

In addition, the 3<sup>rd</sup> order intercept point (  $IP_3$  ) is where the asymptotes for the 3<sup>rd</sup> order inter-modulation product and the fundamental meet.  $IIP_3$  is the input power and  $OIP_3$  is the output power corresponding to the intercept point. They are generally measured in dBm.

Furthermore, it is noted that 1 dB compression point occurs at lower input power than  $IP_3$ . This general relationship is employed in practical approximation for estimation of  $IP_3$  from 1 dB compression point as [Jose, 2004]:

$$IIP_3 \approx P_{1dB,in} + 10dB \quad (2.7)$$

Where  $IIP_3$  indicates the input referred third-order intercept point, and  $P_{1dB,in}$  shows the input referred 1 dB compression point.

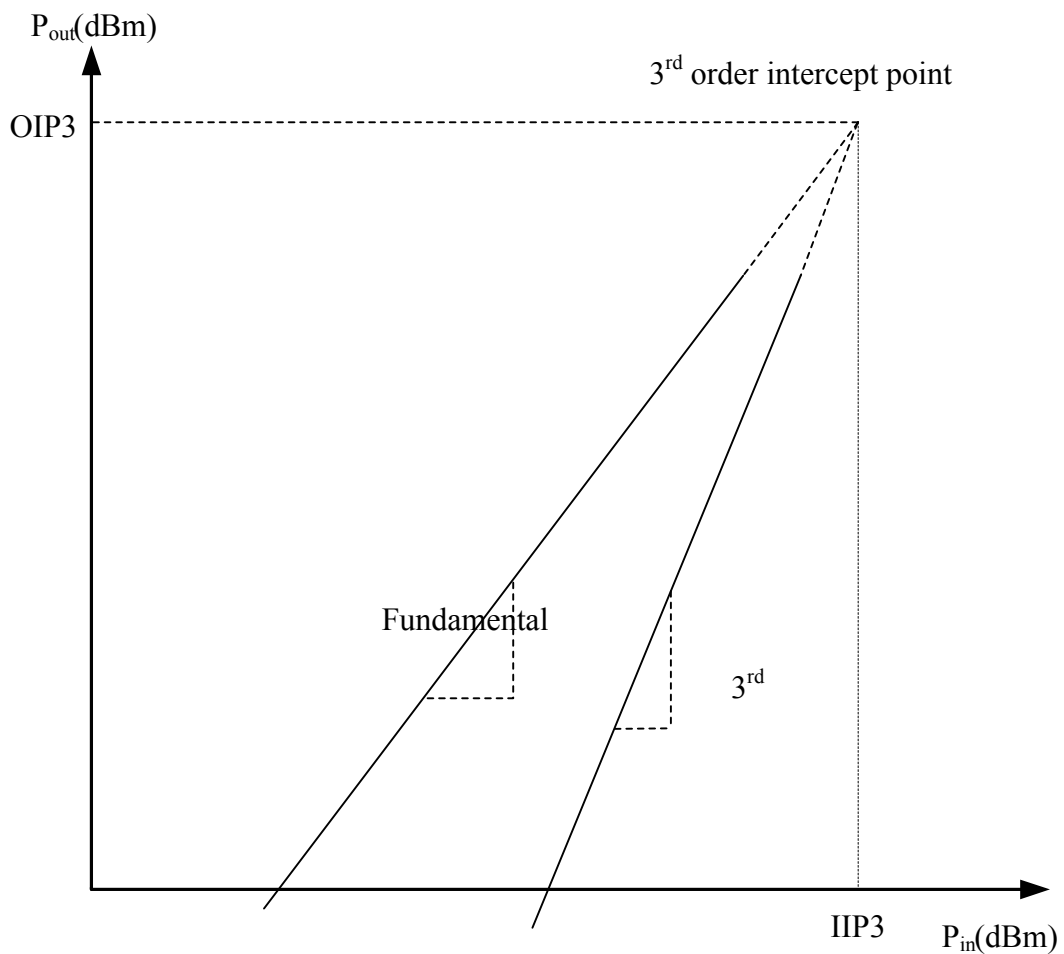


**Fig. 2.4:** The third order intercept point ( $IP_3$ )

## CHAPTER 3

### ULTRA-WIDE BANDWIDTH RECEIVER ARCHITECTURES

The Ultra-wideband (UWB) wireless communication promises a free cabling between consumer electronic devices connectivity, enables gigabytes of data to be transmitted in seconds without exhausting the batteries of hand-held portable devices. The FCC has opened 3.1 GHz to 10.6 GHz spectrum range for unlicensed UWB operation. However, FCC has limited the transmission power to remain below -41 dBm/MHz with hopping frequency of 312.5 ns.

As opposed to narrowband and wideband technologies, UWB transmission is carrier-less. In other words, the data is not modulated with a specific carrier frequency. Therefore, carrier-less transmission requires fewer RF components than carrier based transmission. Hence, the UWB system architecture is significantly simpler as well as cheaper as compared to conventional system architecture.

In this chapter, an overview on UWB system is presented. This is followed by discussions on requirements of receiver. Then, Direct Conversion (DICON) receiver is covered to provide a brief understanding on functionality of each block in the architecture. Finally, this chapter ends with the comparison between the DICON receiver architecture and the Superheterodyne receiver architecture.

#### 3.1 Overview of UWB System

Implementing the receiver chain in the UWB system is a challenging task. The low RF signal level requires the use of low-noise receiver chain while the potential presence of strong out-of-band interferers requires a receiver with high linearity and selectivity. Moreover, the receiver must be able to discriminate the wanted UWB signal, which may be as weak as -70 dBm at a distance of 10m from the transmitter. Besides, it must also be able to discriminate the signal in the presence of a nearby interferer such as an 802.11a at 5 GHz, which the received signal level is around +23 dBm and whose

frequency is only 500 MHz away from the UWB carrier [Leenaerts et al, 2005].

Furthermore, the pressure of reducing the cost and power consumption of communication chips has driven designers to develop transceivers with high-level integration. Achieving the goal of high-level integration is not, however, as simple as replacing external components with on-chip components. Instead, it requires a complete overhaul of the front-end design [Mehta, 2001].

Digital modulation schemes have been used in modern communication systems. Digital modulation provides greater information capacity, higher security and better quality of communication than analogue modulation [Razavi, 1998]. The system's requirements lead to a selection of a receiver.

### **3.2 Requirements of Receiver**

Receivers play role in successfully demodulate a desired signal in the presence of strong interference and noise. The received power is a function of the distance and the surrounding environment between the transmitter and receiver. Thus, it is required that the system has a large dynamic range and low power consumption. There are some requirements of receiver that have to be taken into consideration in order to meet design specifications. They are sensitivity, selectivity, and dynamic range.

Sensitivity of a receiver is defined as the lowest available signal power that a receiver can detect while providing an adequate signal-to-noise ratio (SNR) at the receiver output for demodulation [Rohde and Bucher, 1988]. For a system with digital modulation scheme, the minimum of bit-error-rate (BER) defines the minimum SNR necessary to reproduce the desired signal in satisfactory.

Another key characteristic for a receiver is selectivity. Selectivity is defined as the ability of a receiver to extract the desired signal successfully in the presence of strong adjacent frequency interferers and channel blockers. The selectivity of a receiver relies on the design of channel select filter. It is important to have a receiver that is able to process the signal with an acceptable distortion level. The level of distortion determines the maximum power of an input signal that a receiver can process.

The dynamic range of receiver defines the receiver's ability to detect a weak signal above noise floor and process the large signals with no distortion. The ratio of the maximum signal to the minimum signal at the receiver input defines its dynamic range.

### 3.3 Direct Conversion Architecture (DICON)

Direct conversion (DICON) architecture, shown in Fig. 3.1, has gained popularity in the recent years. In this receiver architecture, the RF signal is mixed with an LO (local oscillator) frequency which is equal to the carrier frequency. Hence, the IF will become zero. Due to this reason, this architecture is also called zero-IF or homodyne architecture.

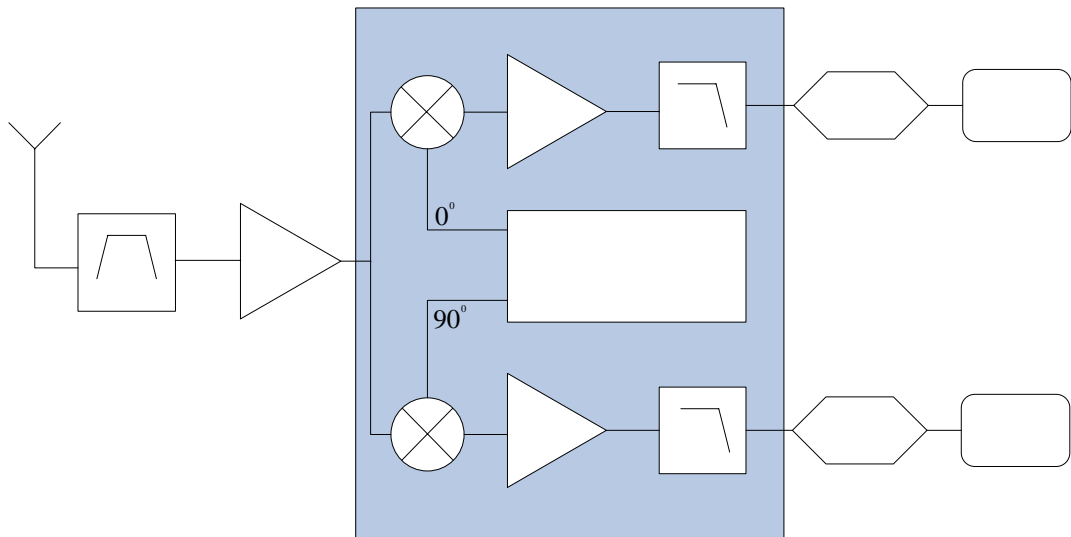


**Fig. 3.1:** Direct Conversion (DICON) Receiver Architecture

The direct conversion architecture offers a number of advantages due to its simplicity in implementation, the possibility of monolithic integration as well as lack of image related problems. Superior integration is due to the fact that no external IF filters or image filters are needed in this architecture. It is also characterized by smaller number of functional blocks than the Superheterodyne receiver. Other resulting

quantities are low power consumption, lower chip area and also lower production cost as compared to the Superheterodyne architecture.

Despite the above-mentioned advantages, direct conversion architecture has some drawbacks. First of all, the second order intermodulation (IP2) requirements for the receiver are high due to direct conversion. Secondly, the system is susceptible to flicker noise especially when it is implemented in CMOS technology. It is due to the fact that low insertion loss passive filters are not available at baseband, and therefore active filter have to be used. Moreover, analog modules running at high frequencies suffer from I/Q imbalance. However, the major challenge deal with direct conversion architecture is DC offset.

A typical Direct Conversion Receiver architecture includes a pre-select filter, a low noise amplifier (LNA), quadrature mixer, followed by variable-gain amplifier (VGA), channel select filters, and analog-to-digital converters. Channel switching time in direct conversion architecture is roughly 10,000 times faster than IEEE 802.11, which is around 2 ns.

In order to achieve multi-band OFDM (Orthogonal Frequency Division Multiplexer) modulation scheme in the three lower bands from 3.1 GHz to 4.9 GHz, the transmission power must be under the FCC limit of -41.25 dBm per Megahertz. Signals transmit at this level is allowed for negligible interference which makes it feasible to develop cost effective CMOS implementation. Moreover, a low noise receiver chain is demanded due to this power limit. This mandates a high linearity and selectivity for the receiver if high data rate transmission is to be successful.

To be more specific about potential interferers in the 2.4 GHz and 5 GHz band, the device must be capable of receiving data from a transmitter 10 meters away in the presence of an 802.11a WLAN transmitter. From the specifications for both devices, it indicates that a -70 dBm UWB signal must be received in the presence of a nearby +23 dBm transmitter operating at a frequency only a few hundreds of MHz away. This poses challenges in the design of receiver front-end over a very large bandwidth with respect to noise and distortion.

Furthermore, it is desirable to limit the dynamic range of subsequent analog-to-digital converters (ADCs). In order to achieve this goal, the interferer should be filtered to a level well below the wanted signal, requiring a wideband IF (intermediate frequency) filter with high attenuation and an accurate and steep roll off.

### **Antenna**

Antenna is the first sub block in the receiver chain. It is a difficult task to produce a high efficiency and matched antenna over a wide bandwidth. The antenna and low noise amplifier should be co-designed in the receiver chain, as low noise amplifier is the subsequent stage after the antenna. Thus, matching issue between the antenna and low noise amplifier has to be taken care in order to achieve full transmission of power without reflection. There are some alternatives for the antenna design, which is from directional and high gain to omnidirectional and low gain antennas. Biconical or bowtie antennas have shown very good performances in the range from 3 GHz to 10 GHz.

### **Pre-select Filter**

A pre-select filter is required after the antenna in the Direct Conversion Receiver architecture. It is required to prevent the out-of-band interferer from entering subsequent stages. Hence, the pre-select filter can help to reduce strong out-of-band interferer.

The pre-select filter or channel select filter must satisfy some requirements such as selectivity, wide dynamic range, and low noise. Due to requirement on selectivity, pre-select filter with sharp cut off is needed. This is because sharp cut off helps in selecting desired channel and attenuate interference. Channel select filter can be implemented with either active components or passive components.

An active implementation of pre-select filter is amenable for on chip integration. However, active filter needs to have as low noise as possible so that it will not to degrade the overall receiver noise figure. Besides, wide dynamic range has to be provided in order to filter out-of-band interferers while do not create intermodulation